Archives of Materials Science and Engineering
Volume 38
Issue 1
July 2009
Pages 12-18
International Scientific Journal published monthly by the World Academy of Materials and Manufacturing Engineering

# Influence of copper addition on properties of $(Fe_{36}Co_{36}B_{19}Si_5Nb_4)_{100-x}Cu_x$ metallic glasses

**S. Lesz [a,*], Z. Stokłosa [b], R. Nowosielski [a]**
[a] Division of Nanocrystalline and Functional Materials and Sustainable Pro-ecological Technologies, Institute of Engineering Materials and Biomaterials, Silesian University of Technology, ul. Konarskiego 18a, 44-100 Gliwice, Poland
[b] Institute of Materials Science, University of Silesia, ul. Bankowa 12, 40-007 Katowice
* Corresponding author: E-mail address: sabina.lesz@polsl.pl

Received 17.03.2009; published in revised form 01.07.2009

## ABSTRACT

**Purpose:** The main aim of the paper was investigation of influence of copper addition on thermal, magnetic and mechanical (microhardness) properties of $(Fe_{36}Co_{36}B_{19}Si_5Nb_4)_{100-x}Cu_x$ (x=0 and 0.6) metallic glasses.

**Design/methodology/approach:** The following experimental techniques were used: differential thermal analysis (DTA), transmission electron microscopy (TEM) and X-ray diffraction (XRD) method, measurements of magnetic properties, Vickers microhardness.

**Findings:** It was shown that addition of small amount of copper to the base alloy induced a change of thermal, magnetic and mechanical properties.

**Research limitations/implications:** The relationship between structure and magnetic and mechanical properties can be useful for practical application of these alloys.

**Practical implications:** The $(Fe_{36}Co_{36}B_{19}Si_5Nb_4)_{100-x}Cu_x$ (x=0 and 0.6) metallic glasses due to a unique properties have been commercialized in the following application fields: precision mould material, precision imprint material, precision sensor material, precision machinery material and surface coating material.

**Originality/value:** The originality of the paper are examinations of changes of thermal and mechanical properties combined with magnetic properties of the $(Fe_{36}Co_{36}B_{19}Si_5Nb_4)_{100-x}Cu_x$ (x=0 and 0.6) metallic glasses.

**Keywords:** Amorphous materials; Thermal properties; Magnetic properties; Mechanical properties; DTA; XRD; TEM method

**Reference to this paper should be given in the following way:**

S. Lesz, Z. Stokłosa, R. Nowosielski, Influence of copper addition on properties of $(Fe_{36}Co_{36}B_{19}Si_5Nb_4)_{100-x}Cu_x$ metallic glasses, Archives of Materials Science and Engineering 38/1 (2009) 12-18.

MATERIALS

## 1. Introduction

Recently, bulk metallic glasses (BMGs) have attracted great attention due to their excellent magnetic and mechanical properties [1-8]. The formation of bulk metallic glasses before 1995 was limited to nonferrous alloy systems [4], an Fe-based bulk metallic glasses was synthesized for the first time in the Fe-(Al, Ga)-metalloid system in 1995 [4,5]. In the past decades until Inoue group developed a series of Fe-based BMGs researches were confirmed. Among BMGs alloys, Fe-based alloys are commercially the most important due not only to the most plentiful natural resources of iron element in the Earth's crust and therefore the less-expensive raw material, but also to the combined of good soft magnetic properties with mechanical and chemical properties. It is well recognized that the low glass-forming ability (GFA) of Fe-based alloys has limited the potential of using them as engineering materials. For this reason extensive efforts have been carried out to improve the GFA of metallic materials and understand the mechanism of effects of various factors on the formation, crystallization, thermal stability and property of BMGs [1-11].

Fe-based ferromagnetic BMGs can be broadly categorized into two groups of types: FePC-based and FeBSi-based alloys [5]. The latter type BMGs , which have been newly developed, exhibit good soft magnetic properties and high mechanical strength, along with high GFA [1,2,4,5,11,12]. For example, in 2004, Inoue at al. have synthesized $[(Fe_xCo_{1-x})_{0.75}B_{0.2}Si_{0.05}]_{96}Nb_4$ (x=0.1,-0.5 at.%) BMGs exhibit good soft magnetic properties, as well as superhigh fracture strength of 3000-4000 MPa and ductile strain of 0.002 [4,5]. With the aim of searching for a Fe-based BMGs with high GFA and excellent magnetic and mechanical properties, the effect of the replacement of Fe by Co and alloying addition have been investigated. The GFA was improved by adding a small amount of some transition metal such as yttrium, nickel, copper, etc. [1-5, 7-12]. Both Shen and Yoshizawa reported that a copper addition causes improvement of the soft magnetic properties [11] Very recently the effect of copper addition on the GFA of $(Fe_{36}Co_{36}B_{19,2}Si_{4,8}Nb_4)_{100-x}Cu_x$ (x=0, 0.5, 0.6, and 1.0 at.%) alloy was studied [11]. It is found that the addition of copper can be positive on the GFA of a FeCo-based alloy. The addition of copper to the base alloy also modifies the solidification behavior of the alloy and induced a change of the thermal properties upon heating [11].

The alloy $Fe_{36}Co_{36}B_{19}Si_5Nb_4$was selected as the base alloy because it has best GFA among the Fe-Co based alloys reported by Shen at al. [4,12]. Further investigations exhibit that among the $(Fe_{36}Co_{36}B_{19,2}Si_{4,8}Nb_4)_{100-x}Cu_x$ (x=0, 0.5, 0.6, and 1.0 at.%) alloy only copper addition equal 0.6 guarantee only one endothermic peak upon melting, which implies that the addition of copper depressed the precipitation of the primary phase. This concentrations of copper allow to obtain good mechanical properties, too [11].

In the present paper influence of copper addition on the thermal, magnetic and mechanical (microhardness) properties of $(Fe_{36}Co_{36}B_{19}Si_5Nb_4)_{100-x}Cu_x$ (x=0 and 0.6 at.%) metallic glasses was investigated. However, many works were dedicated to the results of thermal and mechanical properties investigations, there have been no published data referring to magnetic properties of these alloys with copper addition. In particular interesting is the relationship between structure and magnetic and mechanical properties.

## 2. Experiments

Investigations were carried out on amorphous ribbons with compositions of $(Fe_{36}Co_{36}B_{19}Si_5Nb_4)_{100-x}Cu_x$ (x=0 and 0.6 at.%). The Fe-based master alloy ingots with above compositions were prepared by arc melting the mixtures of the Fe-B , Fe-Nb, Fe-Si starting alloys and pure Fe, Co, Ni metals in an argon atmosphere. The alloy compositions represent nominal atomic percentages. Ribbons with thickness of 0.07 and 0.27 mm and width of 2.3 mm were prepared by the single copper roller melt spinning method. The master alloy was melted in a quartz crucible using an induction coil and pushed thereafter on a copper wheel by applying an ejection pressure of about 200 mBar.

Thermal properties (liquidus -$T_l$ and solidus - $T_s$ temperatures of the pre-alloyed ingots (as well as the base alloy and the alloy with 0.6 at.% copper addition) upon heating and cooling were analyzed by a. NETZSCH model DSC 404 C Pegasus under the purified argon atmosphere, at the heating and cooling rate of 20 K/min.

The microstructure of the ribbons was examined by X-ray diffraction (XRD) and TEM method.

The X-ray method has been performed by the use of diffractometer X-Pert PRO MP with filtered Co-Kα radiation.

In order to conduct structural study, the electron microscope TESLA BS 540 in the range of 52000× to 150000× magnitude was used.

For samples in the as quenched state, the relative magnetic permeability (Maxwell-Wien bridge, frequency 1 kHz, magnetic field 0.5 A/m) at room temperature were obtained.

The measurements of magnetic permeability $\mu_i$ (at force H≈0.5 A/m and frequency f≈1 kHz) and the intensity of magnetic after effect $\Delta\mu/\mu(t_1)$ ($\Delta\mu=\mu(t_1=30\ s)-\mu(t_2=1800\ s)$), where μ is the initial magnetic permeability measured at time t after demagnetisation, have been done. The investigations of tapes in as quenched state were performed with the use of automatic device for measurements magnetic permeability [13,14].

Additionally for ribbons of $Fe_{36}Co_{36}B_{19}Si_5Nb_4$ alloys with thickness of 0.07 mm the saturation magnetization M(T) was measured in situ with heating rates 5K/min with the use of a magnetic balance. The magnetization curve M(T) normalized to the value at 300 K and the corresponding dM/dT curves were presented. The Curie temperature $T_C$ is determined from the condition dM/dT =minimum [8-10,13].

Microhardness was measured with a use of the Vickers hardness tester PMT–3 under a load of 49N (50G) [14]. The microhardness was measured on the shining surface of ribbons according to pattern presented in Figure 1.

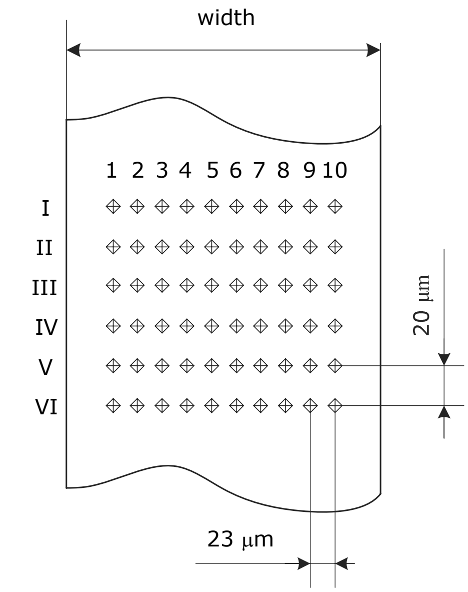


Fig. 1. The pattern of microhardness measurements

## 3. Results and discussion

It was found from the obtained results of structural studies performed by X-ray diffraction, transmission electron microscopy (TEM), that in as quenched state the structure of the ribbons with thickness of both 0.07 mm and 0.27 mm of $(Fe_{36}Co_{36}B_{19}Si_5Nb_4)_{100-x}Cu_x$ (x=0 and 0.6) alloy consists of amorphous phase (Figures 2-6).

The X-ray tests prove that the structure of the all of ribbons as well as $Fe_{36}Co_{36}B_{19}Si_5Nb_4$ and $Fe_{35.75}Co_{35.75}B_{18.90}Si_5Nb_4Cu_{0.6}$ alloy at as quenched state is amorphous, which is seen on the diffraction pattern in the form of a broad-angle peak originating from amorphous phase (Figure 2 a,b).

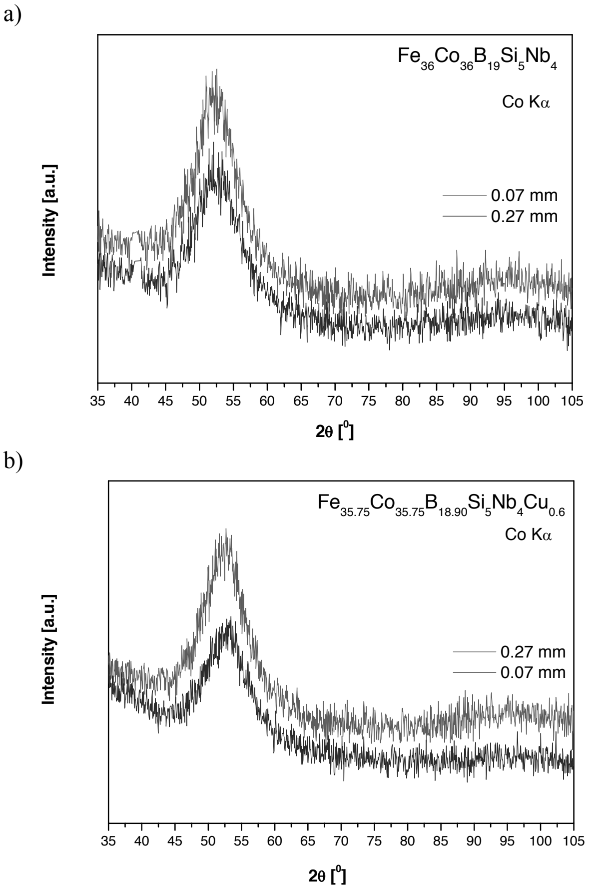


Fig. 2. X-ray diffraction pattern of the $Fe_{36}Co_{36}B_{19}Si_5Nb_4$ (a) and $Fe_{35.75}Co_{35.75}B_{18.90}Si_5Nb_4Cu_{0.6}$ (b) ribbons

Obtained results of structural studies performed by X-ray diffraction are corresponding with the HRTEM micrograph. The diffraction pattern taken from the small region consists only of halo rings, and no appreciable reflection spots of crystalline phases are seen (Figures 3-6).

From DTA, a course of eutectic transformation was determined for a base alloy containing 0.6at% Cu.

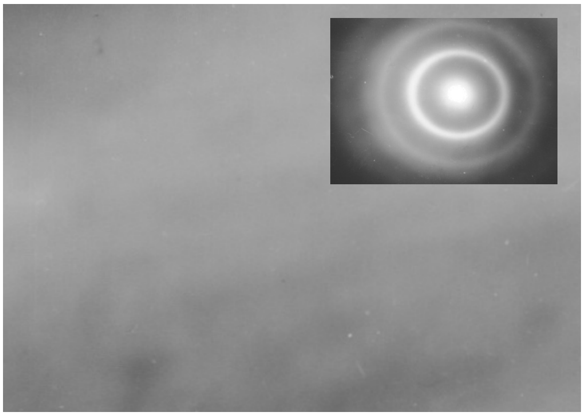

Fig. 3. TEM micrograph and selected area electron diffraction pattern of $Fe_{36}Co_{36}B_{19}Si_5Nb_4$ ribbons with thickness of 0.07 mm in as quenched state. Mag= 100000×

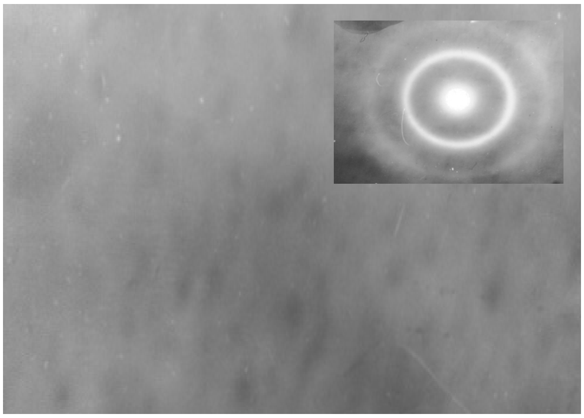

Fig. 4. TEM micrograph and selected area electron diffraction pattern of $Fe_{36}Co_{36}B_{19}Si_5Nb_4$ ribbons with thickness of 0.27 mm in as quenched state. Mag= 100000×

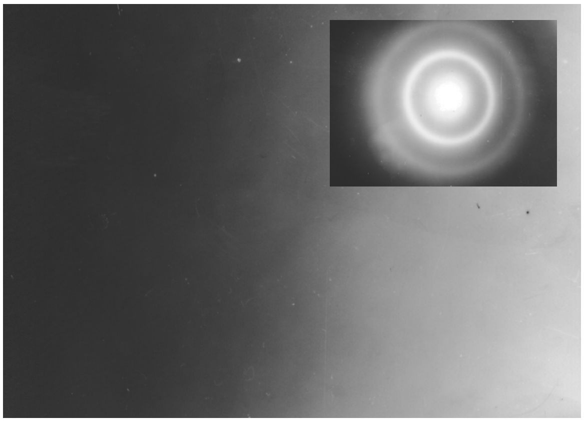

Fig. 5. TEM micrograph and selected area electron diffraction pattern of $Fe_{35.75}Co_{35.75}B_{18.90}Si_5Nb_4Cu_{0.6}$ ribbons with thickness of 0.07 mm in as quenched state. Mag= 150000×

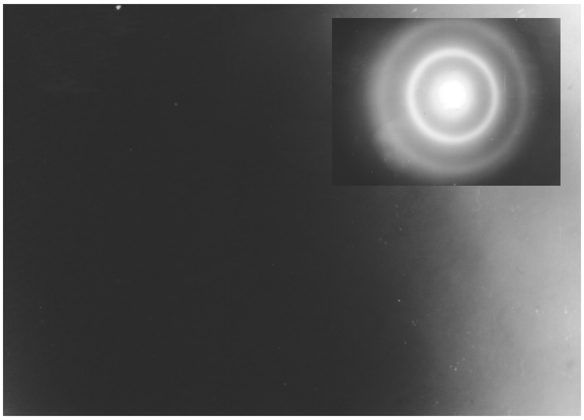

Fig. 6. TEM micrograph and selected area electron diffraction pattern of $Fe_{35.75}Co_{35.75}B_{18.90}Si_5Nb_4Cu_{0.6}$ ribbons with thickness of 0.27 mm in as quenched state. Mag= 52000×

The thermal properties of the pre-alloyed ingots base alloy and the alloy with 0.6 at.% copper addition upon heating measured by DTA are presented on Figure 7.

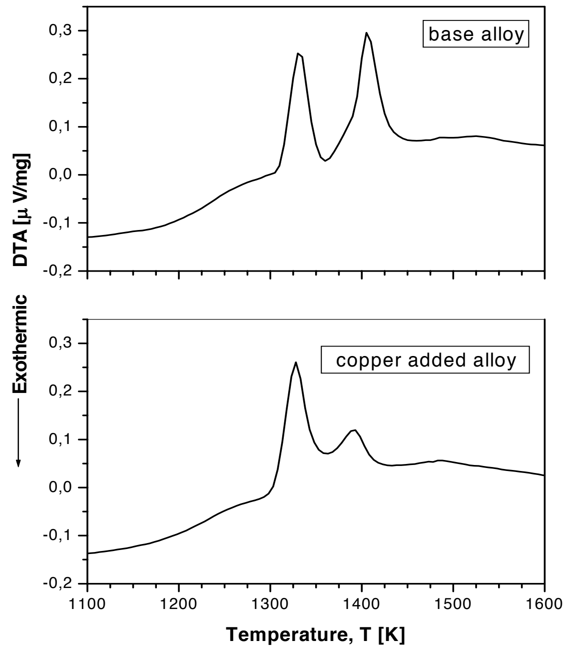


Fig. 7. Differential thermal analysis (DTA) curves of the base master alloy and of the copper added alloy under the heating rate of 20 K/min

On heating, melting requires an input of heat and the peak is endothermic. The base alloy and copper added alloy present clearly two endothermic peaks. The first peak for base alloy begins near the eutectic (melting) point – 1312 K For copper added alloy the onset of melting occurs at the eutectic temperature, 1305 K.

Figure 8 shows thermal properties of the pre-alloyed ingots base alloy and the alloy with 0.6% copper addition upon cooling measured by DTA. For the base alloy two peaks are clearly shown (Figure 8). The first peak corresponds to the eutectic temperature (1294 K) and the maximum signal of the second peak occurs near the liquidus (1393 K). The reason the maximum signal of the second peak is associated with the liquidus temperature will be discussed in [15]. For the alloy with 0.6% at. copper addition only one major peak is observed ($T_{peak}$=1282 K). For these alloy the onset of melting occurs at 1266 K and end at 1303 K. This peak is undoubtedly the eutectic transformation temperature. Y. Jia reported that the copper addition to the base alloy depresses the possibility of the precipitation of the competing phase and thus improved the GFA of the base alloy. The GFA of an alloy is composition - dependent [11].

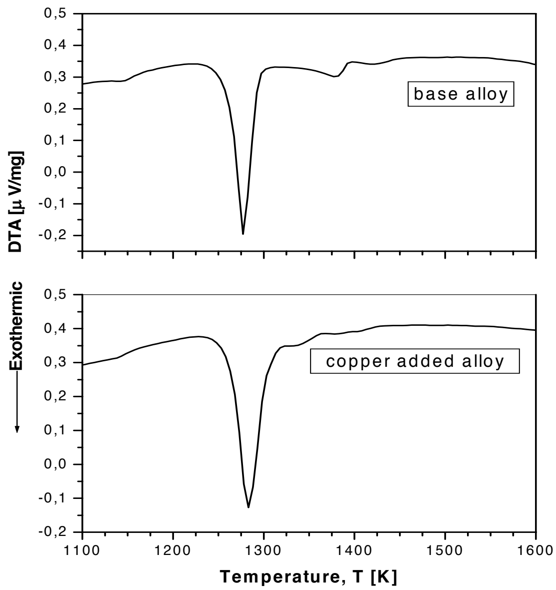


Fig. 8. Differential thermal analysis (DTA) curves of the base master alloy and of the copper added alloy under the cooling rate of 20 K/min

The results of magnetic properties measurements of the investigated ribbons of the $(Fe_{36}Co_{36}B_{19}Si_5Nb_4)_{100-x}Cu_x$ alloys have been presented in the Table 1.

The value of Curie temperature for the $Fe_{36}Co_{36}B_{19}Si_5Nb_4$ ribbons of thickness of 0.07 mm is equal 575 K (Figs. 9, 10). The similar value of $T_c$ was obtained in [10].

The detailed analysis of data of magnetic properties i.e. $\mu_i$ and $H_c$ allow to classify the alloy in as quenched state as a soft magnetic material. (Table 1). The ribbons with thickness of 0.07 mm have better magnetic properties ($H_c$=4,0 A/m, $\mu_i$=3000, $\Delta\mu/\mu$=5.0, Table 1) than ribbons with thickness of 0.27 mm

($H_c$=4.7 A/m, $\mu_i$=390, $\Delta\mu/\mu$=8,0, Table 1) of $Fe_{36}Co_{36}B_{19}Si_5Nb_4$ alloy. The similar relationship was observed in the copper added alloy. The addition of copper to the base alloy improved magnetic permeability $\mu_i$ what probably is connected with impurity content. Y. Jia reported that the copper addition to the base alloy decreased the impurity content [11]. However the coercivity $H_c$ of the base alloy is lower than copper added alloy. In the amorphous alloy, the domain walls are free to move due to the low magnetocrystalline anisotropy, resulting in a low $H_c$. The lower coercivity could be obtained upon heating in order to reduce the stress field in the as-cast amorphous matrix. The addition of copper to the base alloy elongation of the crystallization procedure provides us a chance to obtain nano-structured material with better soft magnetic property by annealing the alloy avoiding the rapid crystallization of the amorphous precursor [11]. However, when there are crystallites or impurities in the alloy, thay can pin the domain walls. This might result in a high coercivity [16].

The thinner ribbons have better magnetic properties, what suggests that the casting conditions have influence on microvoids content and thereby on magnetic properties. These excellent magnetic properties (Table 1) lead us to expect that the Fe-based amorphous alloy could be used as a new engineering and functional material intended for parts of inductive components.

The microvoids content is often examined using magnetic aftereffects ($\Delta\mu/\mu$) measurements. The value of $\Delta\mu/\mu$ increases with increasing of microvoids into materials [13].

The values of $H_c$ and $T_c$ obtained for the ribbons with thickness of 0.07 mm and 0.27 mm of $Fe_{36}Co_{36}B_{19}Si_5Nb_4$ alloy are similar than for these alloys in rod form with 5 mm diameter investigated by B. Shen, A. Inoue [4] whose results as follows: $H_c$=1.5 A/m and $T_c$=692K. Results of microhardness experiments on ribbons with thickness of 0.07 mm and 0.27 mm of the base alloy and the alloy with 0.6% copper addition are presented in Tables 2, 3 and 4, 5, respectively. The results of microhardness measurements points to changeable microhardness of $(Fe_{36}Co_{36}B_{19}Si_5Nb_4)_{100-x}Cu_x$ (x=0 and 0.6) ribbons with thickness of 0.07 mm and 0.27 mm depended on place of measurements.

Microhardness $H_v$ varies between 1413-1789 on the margin of ribbons and 1049-1314 in centre of $Fe_{36}Co_{36}B_{19}Si_5Nb_4$ ribbons (Tables 2, 3). Similary microhardness $H_v$ of $Fe_{35.75}Co_{35.75}B_{18.90}Si_5Nb_4Cu_{0.6}$ alloy varies between 1524-1947 on the margin of ribbons and 1197-1524 in centre of ribbons (Tables 4, 5).

These differences may suggest that process of solidification of amorphous ribbons is different in centre and on the margin and is connected with cooling rate of ribbons during casting.

The values of microhardness of ribbons of $Fe_{36}Co_{36}B_{19}Si_5Nb_4$ considerably exceed values obtained for these alloy in rod form (with 5 mm diameter)- 1220 $H_v$ in [4].

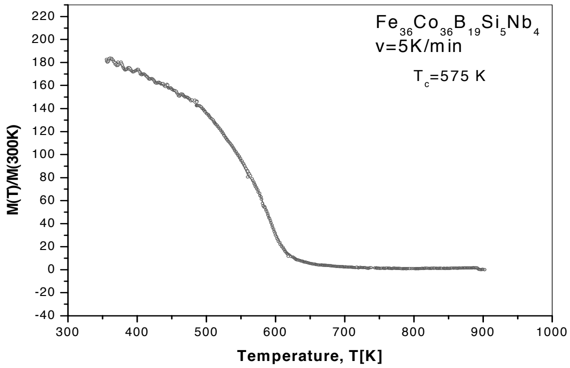


Fig. 9. Normalized magnetization versus temperature *T* of $Fe_{36}Co_{36}B_{19}Si_5Nb_4$ ribbons with thickness of 0.07 mm

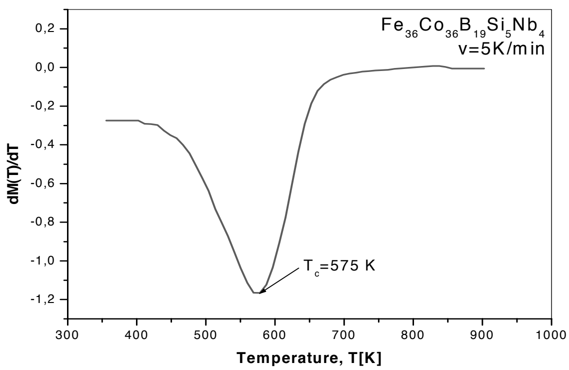


Fig. 10. dM(T)/dT curves for the data presented in Fig. 9

Table 1.
Magnetic properties ($\mu_i$ –initial magnetic permeability, $\Delta\mu/\mu$ - magnetic after effects, $H_c$ – coercivity) of $(Fe_{36}Co_{36}B_{19}Si_5Nb_4)_{100-x}Cu_x$ ribbons with thickness of 0.07 mm and 0.27 mm

| Composition of alloys | Thickness of ribbons | | Magnetic properties | |
|---|---|---|---|---|
| [at. %] | [mm] | $\mu_i$ | $\Delta\mu/\mu$ [%] | $H_c$ [A/m] |
| $Fe_{36}Co_{36}B_{19}Si_5Nb_4$ | 0.07 | 3000 | 5 | 4.0 |
| $Fe_{36}Co_{36}B_{19}Si_5Nb_4$ | 0.27 | 390 | 8 | 4.7 |
| $Fe_{35.75}Co_{35.75}B_{18.90}Si_5Nb_4Cu_{0.6}$ | 0.07 | 3620 | 11 | 4.8 |
| $Fe_{35.75}Co_{35.75}B_{18.90}Si_5Nb_4Cu_{0.6}$ | 0.27 | 820 | 10 | 16 |

Table 2.
Results of microhardness experiments (see Fig. 1) of $Fe_{36}Co_{36}B_{19}Si_5Nb_4$ ribbons with thickness of 0.07 mm

| No. | 1 | 2 | 3 | 4 | 5 | 6 | 7 | 8 | 9 | 10 |
|---|---|---|---|---|---|---|---|---|---|---|
| I | 1648 | 1648 | 1413 | 1524 | 1197 | 1648 | 1413 | 1648 | 1648 | 1648 |
| II | 1648 | 1413 | 1524 | 1413 | 1314 | 1197 | 1314 | 1413 | 1524 | 1789 |
| III | 1524 | 1413 | 1413 | 1413 | 1197 | 1197 | 1314 | 1524 | 1648 | 1648 |
| IV | 1413 | 1648 | 1648 | 1413 | 1314 | 1314 | 1413 | 1524 | 1789 | 1789 |
| V | 1648 | 1413 | 1524 | 1413 | 1197 | 1314 | 1314 | 1413 | 1648 | 1648 |
| VI | 1524 | 1413 | 1413 | 1524 | 1314 | 1197 | 1314 | 1524 | 1524 | 1648 |

Table 3.
Results of microhardness experiments (see Fig. 1) of $Fe_{36}Co_{36}B_{19}Si_5Nb_4$ ribbons with thickness of 0.27 mm

| No. | 1 | 2 | 3 | 4 | 5 | 6 | 7 | 8 | 9 | 10 |
|---|---|---|---|---|---|---|---|---|---|---|
| I | 1648 | 1648 | 1648 | 1413 | 1197 | 1120 | 1197 | 1314 | 1413 | 1413 |
| II | 1524 | 1413 | 1413 | 1314 | 1120 | 1120 | 1413 | 1197 | 1524 | 1524 |
| III | 1413 | 1524 | 1413 | 1197 | 1049 | 1120 | 1314 | 1314 | 1413 | 1648 |
| IV | 1413 | 1413 | 1314 | 1314 | 1120 | 1120 | 1314 | 1314 | 1524 | 1524 |
| V | 1413 | 1524 | 1413 | 1314 | 1197 | 1120 | 1197 | 1197 | 1413 | 1648 |
| VI | 1524 | 1413 | 1314 | 1197 | 1197 | 1197 | 1314 | 1524 | 1524 | 1648 |

Table 4.
Results of microhardness experiments (see Fig. 1) of $Fe_{35.75}Co_{35.75}B_{18.90}Si_5Nb_4Cu_{0.6}$ ribbons with thickness of 0.07 mm

| No. | 1 | 2 | 3 | 4 | 5 | 6 | 7 | 8 | 9 | 10 |
|---|---|---|---|---|---|---|---|---|---|---|
| I | 1648 | 1648 | 1524 | 1314 | 1524 | 1197 | 1413 | 1789 | 1648 | 1789 |
| II | 1648 | 1648 | 1524 | 1413 | 1314 | 1314 | 1524 | 1789 | 1789 | 1648 |
| III | 1648 | 1789 | 1648 | 1413 | 1524 | 1314 | 1524 | 1524 | 1648 | 1648 |
| IV | 1648 | 1789 | 1413 | 1524 | 1413 | 1524 | 1524 | 1789 | 1648 | 1789 |
| V | 1648 | 1648 | 1524 | 1648 | 1413 | 1413 | 1648 | 1524 | 1789 | 1789 |
| VI | 1789 | 1524 | 1413 | 1524 | 1413 | 1524 | 1648 | 1648 | 1648 | 1789 |

Table 5.
Results of microhardness experiments (see Fig. 1) of $Fe_{35.75}Co_{35.75}B_{18.90}Si_5Nb_4Cu_{0.6}$ ribbons with thickness of 0.27 mm

| No. | 1 | 2 | 3 | 4 | 5 | 6 | 7 | 8 | 9 | 10 |
|---|---|---|---|---|---|---|---|---|---|---|
| I | 1648 | 1413 | 1314 | 1413 | 1197 | 1413 | 1524 | 1789 | 1648 | 1947 |
| II | 1648 | 1648 | 1314 | 1314 | 1197 | 1524 | 1413 | 1524 | 1648 | 1648 |
| III | 1789 | 1524 | 1413 | 1314 | 1314 | 1314 | 1413 | 1789 | 1648 | 1789 |
| IV | 1947 | 1789 | 1648 | 1524 | 1413 | 1314 | 1413 | 1524 | 1524 | 1648 |
| V | 1789 | 1789 | 1524 | 1314 | 1413 | 1524 | 1413 | 1789 | 1648 | 1789 |
| VI | 1947 | 1648 | 1648 | 1413 | 1314 | 1413 | 1413 | 1789 | 1789 | 1648 |

## 4. Conclusions

We can state that the structure of the all of ribbons as well as $Fe_{36}Co_{36}B_{19}Si_5Nb_4$ and $Fe_{35.75}Co_{35.75}B_{18.90}Si_5Nb_4Cu_{0.6}$ alloy at as quenched state is amorphous. The object of this study were alloys in ribbons form 1000% thicker than classical ribbons (thickness ~0.03 mm).

The addition of small amount of copper to the base alloy induced a change of thermal, magnetic and mechanical properties. The addition of small amounts of Cu slightly changes of microhardness but is very effective in changing thermal properties and magnetic properties.

The melting temperature $T_m$ remained almost constant for both investigated alloy. Two alloy compositions are at or very close to the eutectics. According to ref. [3], the best metallic glass-forming alloys are at or near deep eutectic composition.

The investigated alloys have good soft magnetic properties. The value of Curie temperature for the $Fe_{36}Co_{36}B_{19}Si_5Nb_4$ ribbons with thickness of 0.07 mm is equal 575 K. Thinner ribbons of $(Fe_{36}Co_{36}B_{19}Si_5Nb_4)_{100-x}Cu_x$ alloys exhibit better soft magnetic properties than the other ribbon. Magnetic permeability $\mu_i$ of ribbons of copper added alloy are better than base alloy. However values of $H_c$ of thicker ribbons of copper added alloy considerably exceed values obtained for base alloy.

These excellent magnetic properties lead us to expect that the investigated amorphous alloy is promising for the future applications as new engineering and functional material on the parts of micromotors and other applications.

Results of microhardness measurements proved that a small amount of copper addition has slight influence on $H_v$ values of the Fe-Co based alloy. Microhardness $H_v$ varies between 1413-1789 on the margin of ribbons and 1049-1314 in centre of $Fe_{36}Co_{36}B_{19}Si_5Nb_4$ ribbons. Similary microhardness $H_v$ of $Fe_{35.75}Co_{35.75}B_{18.90}Si_5Nb_4Cu_{0.6}$ alloy varies between 1524-1947 on the margin of ribbons and 1197-1524 in centre of ribbons. The microhardness changes on the surface of ribbons can suggest that process of solidification of ribbons influence on amorphization process.

The present Fe-Co based metallic glasses with high GFA and high microhardness may promise extraordinary application potential as structural materials.

The results obtained for the melt-spun glassy alloy ribbons are the beans for continuation of research on different forms of the investigated alloy, i.e. rods or tubes.

## Acknowledgements

This work was supported by Polish Ministry of Science (grant N507 027 31/0661).

## References

[1] A. Inoue, B.L. Shen, C.T. Chang, Fe- and Co-based bulk glossy alloys with ultrahigh strength of over 4000 MPa, Intermetallics 14 (2006) 936-944.

[2] A. Inoue, B. Shen, A. Takeuchi, Fabrication, properties- and applications of bulk glassy alloys in late transition metal-based systems, Materials Science and Engineering A 441 (2006) 18-25.

[3] W.H. Wang, Roles of minor additions in formation and properties of bulk metallic glasses, Progress in Materials Science 52 (2007) 540-596.

[4] B. Shen, A. Inoue, Superhigh strength and good soft-magnetic properties of (Fe,Co)-B-Si-Nb bulk glassy alloys with high glass-forming ability, Applied Physics Letters 85/21 (2004) 4911-4913.

[5] Z.L. Long, Y. Shao, X.H. Deng, Z.C. Zhang, Y. Jiang, P. Zhang, B.L. Shen, A. Inoue, Cr effect on magnetic and corrosion properties of Fe-Co-Si-B-Nb-Cr bulk glassy alloys with high glass forming ability, Intermetallics 15 (2007) 1453-1458.

[6] K.F. Yao, C.Q. Zhang, Fe-based bulk metallic glass with high plasticity, Applied Physics Letters 90 (2007) 061901.

[7] Ch. Chang, B. Shen, A. Inoue, FeNi-based bulk glassy alloys with superhigh mechanical strength and excellent soft magnetic properties, Applied Physics Letters 89 (2006) 051912.

[8] S. Lesz, P. Kwapuliński, R. Nowosielski, Formation and physical properties of Fe-based bulk metallic glasses with Ni addition, Journal of Achievements in Materials and Manufacturing Engineering 31/1 (2008) 35-40.

[9] R. Nowosielski, R. Babilas, P. Ochin, Z. Stokłosa, Thermal and magnetic properties of selected Fe-based metallic glasses, Archives of Materials Science and Engineering 30/1 (2008) 13-16.

[10] R. Nowosielski, R. Babilas, Structure and magnetic properties of Fe36Co36B19Si5Nb4 bulk metallic glasses, Journal of Achievements in Materials and Manufacturing Engineering 30/2 (2008) 135-140.

[11] Y. Jia, S. Zeng, S. Shan, L. Zhang, C. Fan, B. Zhang, Z. Zhan, R. Liu, W. Wang, Effect of copper addition on the glass forming ability of a Fe-Co based alloy, Journal of Alloys and Compounds 440 (2007) 113-116.

[12] B. Shen, C. Chang, A. Inoue, Formation, ductile deformation behavior and soft – magnetic properties of (Fe, Co, Ni)-B-Si-Nb bulk glassy alloys, Intermetallics 15 (2007) 9-16.

[13] P. Kwapuliński, J. Rasek, Z. Stokłosa, G. Badura, B. Kostrubiec, G. Haneczok, Magnetic and mechanical properties In FeXSiB (X=Cu,Zr,Co) amorphous alloys, Archives of Materials Science and Engineering 31/1 (2008) 25-28.

[14] Polish standard: PN – EN ISO 6507 - 1:2007.

[15] W.J. Boettinger, U.R. Kattner, K.-W. Moon, J.H. Perepezko, DTA and Heat flux DSC Measurements of Alloy Melting and Freezing, National Institute of Standards and Technology Special Publication 960/15 (2006).

[16] W.S. Sun, T. Kulik, X.B. Liang, J. Ferenc, Thermal stability and magnetic properties of Co-Fe-Hf-Ti-Mo-B bulk metallic glass, Intermetallics 14 (2006) 1066-1068.